Contribution from the Department of Chemistry and Centre for Chemical Physics, University of Western Ontario, London, Ontario, Canada, and Department of Chemistry, McMaster University, Hamilton, Ontario, Canada

Theoretical and Experimental Shake-up Studies of KrF_2, XeF_4, and XeF_6[1]

G. M. BANCROFT,*[2a] D. J. BRISTOW,[2a,b] J. S. TSE,[2a,c] and G. J. SCHROBILGEN[2d]

Received January 14, 1983

The X-ray photoelectron spectra of core levels of KrF_2, XeF_4, and XeF_6 have been obtained. We observe a number of satellites on the low kinetic energy side of these core levels, and these satellites have been assigned to monopole-allowed shake-up transitions by using Xα–SW hole state calculations and atomic model calculations. Calculated energies are generally in reasonable agreement with observed values, and the calculated intensities for the low-energy shake-up transitions in KrF_2 are in good agreement with the observed intensities. An Xα–SW calculation on the KrF_2 ground state gives good agreement with the experimental valence-band energies.

Introduction

There have been a number of recent spectroscopic studies on the Xe fluorides, XeF_2, XeF_4, and XeF_6,[3] but there has been less interest in the very unstable krypton analogue KrF_2. However, the He I and He II photoelectron spectra of KrF_2 have been obtained,[4] and the molecular orbital scheme has been derived from these spectra and theoretical calculations.[4-6] The KrF_2 electronic structure is strikingly similar to that of the XeF_2 analogue.[4]

We have been interested in characterizing the shake-up spectra of rare gas atoms[7] and molecules.[3] In our previous work on XeF_2, we were able to interpret the Xe 3d shake-up spectra using SCF–Xα–SW calculations[3] and a rather novel simple atomic model first used by Lindholm,[8] which gave suprisingly good predictions for the shake-up energies.

In this paper, we concentrate our attention on the KrF_2 shake-up spectra but also report the Xe 4d and Xe 3d shake-up spectra of XeF_4 and XeF_6, respectively. We are able to assign the Kr 3d and F 1s shake-up spectra readily using Xα calculations and the atomic model. The valence orbital energies from a ground-state Xα calculation are in better agreement with the observed photoelectron energies than previous theoretical calculations.

Experimental Section

The compounds KrF_2, XeF_4, and XeF_6 were all synthesized by Schrobilgen using referenced methods.[9,10] Spectra were obtained on a McPherson 36 photoelectron spectrometer using either Mg Kα (KrF_2) or Al Kα (XeF_4, XeF_6) sources to circumvent the problem of overlapping Auger peaks.

Decomposition, especially with KrF_2, was considerable using the standard McPherson stainless gas-inlet system. For this reason we constructed an inlet system out of Kel-F except the sample cell itself. Minimal decomposition was detected with this setup. All of the rare-gas fluorides have adequate vapor pressure at room temperature for easy collection of the spectra. KrF_2 however is unstable at room temperature and thus had to be kept cold during data acquisition. We found that a hexanol/liquid N_2 bath (~−50 °C) was perfect for this purpose. At this temperature the Kel-F valves could be opened wide, and the KrF_2 vapor pressure was just adequate for reasonable statistics. KrF_2 and XeF_6 degraded our channeltron detectors rapidly; and thus the spectra of these two compounds could not be multiscanned as long as for XeF_2 to obtain comparable statistics.

The gas pressure in our gas cell, although not measured directly, is not high enough to observe satellites due to inelastic scattering. For example, shake-up spectra of CH_4[11] obtained in this laboratory do not show the inelastic peak and shoulder at 9.9 and 15 eV, respectively, seen by Pireaux et al.[12] However, we cannot totally rule out inelastic peaks for these molecules. The spectra were fit by a least-squares program written by Coatsworth[13] and modified to constrain spin–orbit doublets by R. P. Gupta. The shake-up intensities were calculated with an Xα program written by G. Loubriel[14] and modified by J.S.T. to operate on our computer system.

Results and Discussion

(a) KrF_2. The Kr 3d and F 1s shake-up spectra of KrF_2 are shown in Figures 1 and 2, respectively. The Kr 3d shake-up spectra have been fit to spin–orbit doublets, with the energy separation and intensity ratio of the doublets constrained to the values from the Kr 3d primary line. The experimental and theoretical energies and intensities along with the assignments are listed in Tables I and II. These assignments have been made with the aid of the Xα and atomic model calculations.

We have carried out Xα–SW calculations on the ground state and Kr 3d and F 1s hole states of KrF_2. The parameters employed are listed in Table III, and the highest l values used in the basic functions are 3, 3, and 2 for the outer, krypton, and fluorine spheres, respectively. The percent orbital character and energy eigenvalues for the ground and Kr 3d hole states appear in Table IV. We have lowered the symmetry to $C_{\infty v}$ for the F 1s hole state (Table V) since theoretical work has found that deep core holes are best described as localized on a single atom.[15] The orbital numbering has been changed to accommodate $C_{\infty v}$ symmetry. However, the origin of the orbitals in the lower symmetry can be traced back to $D_{\infty h}$ symmetry since their ground-state energies are identical (e.g., $6\sigma_g \equiv 9\sigma$). This equivalence of course does not apply for the F 1s hole state, where the fluorines are now inequivalent. A molecular orbital diagram for the two hole states is given in Figure 3. The left side of the diagram corresponds to the situation with a Kr 3d hole while that on the right represents

(1) Presented in part at the VIth Vacuum Ultraviolet Radiation Conference, University of Virginia, Charlottsville, VA, 1980.
(2) (a) University of Western Ontario. (b) Present address: Research Department, Imperial Oil Ltd., Sarnia, Ontario, Canada. (c) Present address: Chemistry Division, National Research Council, Ottawa, Canada. (d) McMaster University.
(3) J. S. Tse, D. J. Bristow, G. M. Bancroft, and G. J. Schrobilgen, *Inorg. Chem.*, **18**, 1766 (1979), and references therein.
(4) C. R. Brundle and G. R. Jones, *J. Chem. Soc., Faraday Trans. 2*, **68**, 959 (1972).
(5) P. S. Bagus, B. Liu, and H. F. Schaefer III, *J. Am. Chem. Soc.*, **94**, 6635 (1972).
(6) R. L. DeKock, *J. Chem. Phys.*, **58**, 1267 (1973).
(7) D. J. Bristow, J. S. Tse, and G. M. Bancroft, *Phys. Rev. A*, **25**, 1 (1982).
(8) E. Lindholm, *Ark. Fys.*, **40**, 97 (1969).
(9) J. G. Malm and C. L. Chernick, *Inorg. Synth.*, **8**, 254, 258, (1966).
(10) R. J. Gillespie and G. J. Schrobilgen, *Inorg. Chem.*, **13**, 1230 (1974).
(11) D. K. Creber, J. S. Tse, and G. M. Bancroft, *J. Chem. Phys.*, **72**, 4291 (1980).
(12) J. J. Pireaux, S. Svensson, E. Basilier, P. A. Malmquist, U. Gelius, R. Caudano, and K. Siegbahn, *Phys. Rev. A*, **14**, 2133 (1976).
(13) G. M. Bancroft, I. Adams, L. L. Coatsworth, C. D. Bennewitz, J. D. Brown, and W. D. Westwood, *Anal. Chem.*, **47**, 586 (1975).
(14) G. Loubriel, Ph.D. Thesis, University of Pennsylvania, 1979.
(15) P. S. Bagus, and H. F. Schaeffer III, *J. Chem. Phys.*, **56**, 224 (1972); H. Ågen, P. S. Bagus, and B. O. Roos, *Chem. Phys. Lett*, **82**, 505 (1981).

0020-1669/83/1322-2673$01.50/0

Table I. KrF_2 Kr 3d Shake-up

line no.	transition	exptl ΔE, eV	exptl intens,[a] %	theor[a] ΔE(Xα-SW), eV	theor[a] ΔE(atomic model), eV	theor[a] intens,[b] %
1	$5\sigma_u \rightarrow 6\sigma_u$	8.4 ± 0.5	9.8	10.3	12.5	9.8
2	$2\pi_g \rightarrow 3\pi_g^*$	16.5 ± 2.0	2.4	14.2		0.4
3	$3\pi_u \rightarrow 5\pi_u^*$ (5p)	19.6 ± 2.0	2.5	19.6	23.3	3.7
4	$5\sigma_u \rightarrow 7\sigma_u^*$	22.4 ± 2.0	2.3	22.0	24.1	0.1
5	$7\sigma_g \rightarrow 9\sigma_g^*$ (5s)	28.1 ± 1.0	3.4	29.9	33.7	0.1
6	$4\sigma_u \rightarrow 7\sigma_u^*$	35.1 ± 1.0	1.5	34.9	40.3	0.03

[a] Uncertainties in the Xα-SW energies and intensities are at least ±1 eV and 10%, respectively. [b] Relative to the primary Kr 3d peaks.

Table II. KrF_2 F 1s Shake-up

line no.	transition	exptl ΔE, eV	exptl intens,[a] %	theor ΔE, eV	theor intens,[a] %
1	$12\sigma \rightarrow 14\sigma^*$	10.2 ± 0.5	12.9	14.3	13.0
2	$6\pi \rightarrow 8\pi^*$	13.4 ± 0.5	5.9	15.5	2.1
	$6\pi \rightarrow 7\pi^*$			14.2	0.6
3	$5\pi \rightarrow 8\pi^*$	16.3 ± 0.5	4.9	17.0	0.4
	$5\pi \rightarrow 7\pi^*$			15.7	0.1
4	$4\pi \rightarrow 8\pi^*$	17.9 ± 0.5	3.1	25.2	0.4
	$4\pi \rightarrow 7\pi^*$			23.8	0.1
	$10\sigma \rightarrow 14\sigma^*$			24.3	0.2

[a] Relative to the primary F 1s peak.

Table III. Parameters Used in the Xα-SW Calculation (au)

region	X	Y	Z	R	α
Kr	0.0	0.0	0.0	2.0301	0.705 74
F	0.0	0.0	3.61	1.5799	0.737 320
F	0.0	0.0	−3.61	1.5799	0.737 320
outer	0.0	0.0	0.0	5.1899	0.725 478

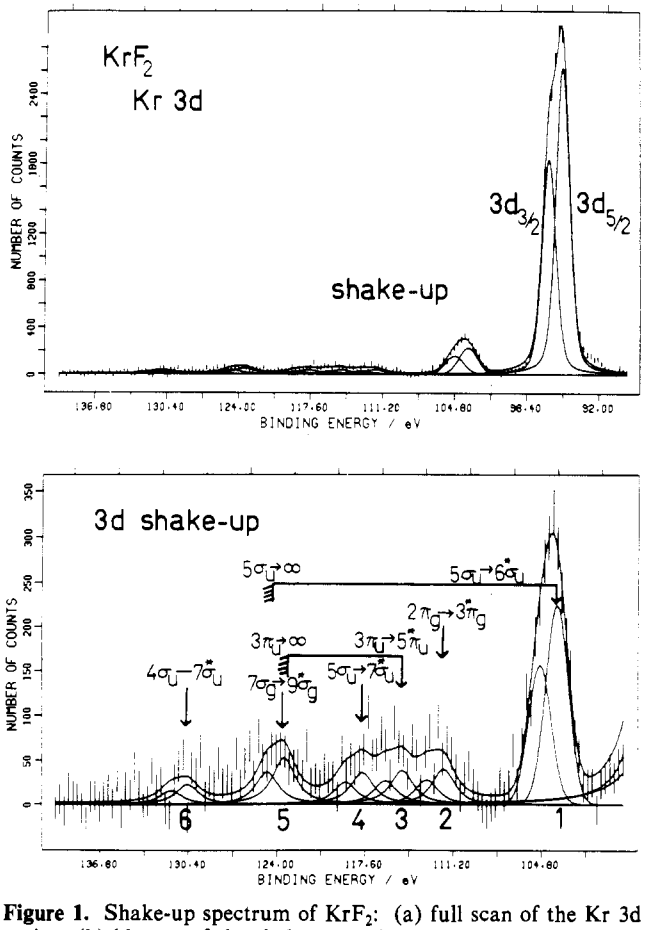

Figure 1. Shake-up spectrum of KrF_2: (a) full scan of the Kr 3d region; (b) blowup of the shake-up region.

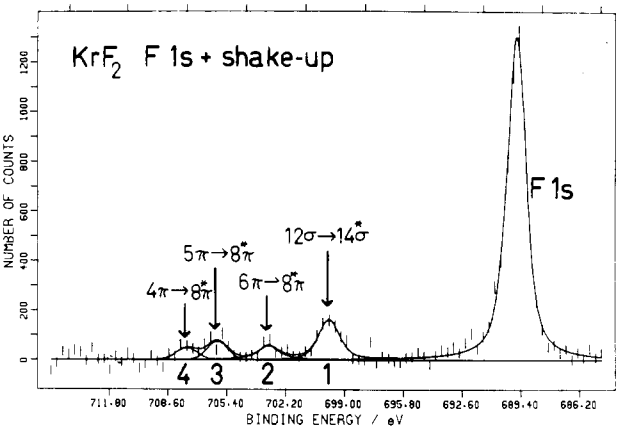

Figure 2. Shake-up spectrum of the F 1s orbital in KrF_2.

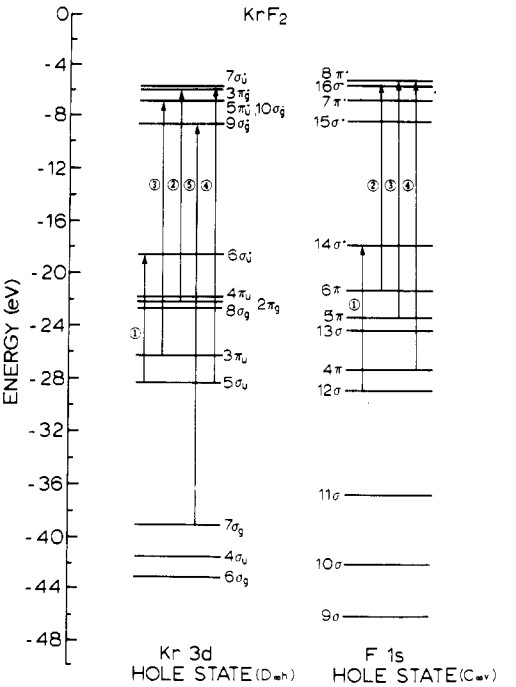

Figure 3. Molecular orbital digrams derived from Xα-SW calculations for the Kr 3d and F 1s hole states in KrF_2.

the energy ordering with a F 1s hole.

Before discussing the shake-up further, it is worthwhile to test the accuracy of the Xα method by calculating the valence binding energies for KrF_2 and comparing these with the experimental values[4] and other theoretical calculations (Table VI). In general, the present calculation provides better agreement with experiment than the previous calculations. All three calculations are in very poor agreement with the $7\sigma_g$ (Kr 4s) orbital at 23.0 eV. A subsequent analysis[6] of the original spectrum[4] suggests that in fact this broad peak is most likely the result of configuration interaction.

Table IV. Calculated Eigenvalues (Ry) and Charge Distribution (%) for KrF_2 Ground State $D_{\infty h}$ and 3d Hole State Valence Molecular Orbitals

	ground state					hole state				
orbital	energy, Ry	outer %	Kr %	F %	inter %	energy, Ry	outer %	Kr %	F %	inter %
$6\sigma_g$	−2.494	0.22	17.92 (s)	80.25 (s)	1.60	−3.159	0.08	53.04 (s)	46.25 (s)	0.63
$7\sigma_g$	−2.099	0.14	75.74 (s)	20.27 (s)	3.86	−2.878	0.20	43.84 (s)	52.85 (s)	0.31
$8\sigma_g$	−1.062	1.31	11.78 (d)	85.53 (p)	1.38	−1.662	0.95	11.73 (d)	87.20 (p)	0.12
$9\sigma_g$*						−0.645	23.44 (s)	0.63	1.09	69.17
$10\sigma_g$*						−0.517	14.21 (d)	29.14 (d)	0.34	56.31
$2\pi_g$	−1.068	0.41	1.81	88.12 (p)	10.17	−1.633	0.26	1.39	89.65 (p)	8.70
$3\pi_g$*						−0.444	13.93 (d)	31.77 (d)	7.25 (p)	47.04
$4\sigma_u$	−2.463	0.35	5.72 (p)	96.61 (s)	1.32	−3.048	0.28	7.24 (p)	91.85 (s)	0.62
$5\sigma_u$	−1.382	0.87	45.34 (p)	54.99 (p)	1.20	−2.083	0.49	59.03 (p)	42.40 (p)	0.0
$6\sigma_u$*						−1.359	1.14	33.43 (p)	62.40 (p)	3.04
$7\sigma_u$*						−0.436	45.80 (p)	1.50	2.78	49.9
$3\pi_u$	−1.184	0.24	56.97 (p)	28.00 (p)	14.78	−1.934	0.03	84.49 (p)	5.22 (p)	10.26
$4\pi_u$	−0.997	0.41	28.45 (p)	62.43 (p)	8.71	−1.604	0.38	6.17 (p)	86.40 (p)	7.06
$5\pi_u$*						−0.515	37.49 (p)	2.76 (p)	0.86	58.89

Table V. Calculated Eigenvalues (Ry) and Charge Distribution (%) for KrF_2 Ground State $C_{\infty v}$ and F 1s Hole State Valence Molecular Orbitals

	ground state						hole state					
orbital	energy, Ry	outer %	Kr %	F* %	F %	inter %	energy, Ry	outer %	Kr %	F* %	F %	inter %
9σ	−2.494	0.22	17.92 (s)	39.53 (s)	40.73 (s)	1.60	−3.368	0.18	4.86 (s)	94.21 (s)	0.012	0.74
10σ	−2.463	0.35	5.72 (p)	46.90 (s)	45.70 (s)	1.32	−3.073	0.23	11.23 (s)	0.20	87.37 (s)	0.96
11σ	−2.099	0.14	75.74 (s)	10.14 (s)	10.12 (s)	3.86	−2.692	0.08	81.03 (s)	6.46 (p)	9.46 (s)	2.97
12σ	−1.382	0.87	45.34 (p)	27.46 (p)	27.53 (p)	1.21	−2.113	0.58	26.41 (p)	66.00 (p)	8.94 (p)	1.92
13σ	−1.062	1.31	11.78 (d)	42.77 (p)	42.75 (p)	1.38	−1.788	0.68	25.02 (p)	20.66 (p)	53.39 (p)	0.25
14σ*							−1.316	0.72	51.55 (p)	10.09 (p)	33.50 (p)	4.14
15σ*							−0.621	26.46 (s)	4.76 (s)	0.53	0.51	67.74
16σ*							−0.428	48.26 (p)	1.75	1.52	1.34	47.13
4π	−1.184	0.24	56.97 (p)	13.95 (p)	14.06 (p)	14.78	−1.998	0.14	2.34	92.22 (p)	0.03	5.28
5π	−1.068	0.41	1.31	43.91 (p)	44.21 (p)	1.02	−1.712	0.15	47.49 (p)	1.63	39.10 (p)	11.62
6π	−0.997	0.41	28.45 (p)	31.42 (p)	31.01 (p)	8.71	−1.596	0.19	38.13 (p)	0.96	52.07 (p)	8.65
7π*							−0.497	40.30 (p)	3.38	0.37	0.28	55.68
8π*							−0.405	26.01 (d)	16.75 (d)	2.49	2.93	51.82

Table VI. Experimental and Theoretical Valence Orbital Energies (eV) of KrF_2

		theor		
orbital	exptl	Xα–SW (this work)	ref 4	ref 5
$4\pi_u$	13.34 13.47	13.56	10.5	15.43
$8\sigma_g$	13.90	14.57	7.9	14.71
$2\pi_g$	14.37	14.53	12.6	17.64
$3\pi_u$	16.92	16.11	15.0	19.36
$5\sigma_u$	17.7	18.80	16.1	20.85
$7\sigma_g$	23.0	28.56	29.0	33.77
$4\sigma_u$	not obsd	33.51		
$6\sigma_g$	not obsd	33.94		

For this reason and because of the good agreement observed for the other valence levels with the Xα–SW calculation, we have employed the theoretical binding energy for the $7\sigma_g$ orbital in the KrF_2 MO diagram based on the atomic model (Figure 4). Photoelectron spectra have been used to position the ground-state Kr[4,16] and KrF_2[4] valence orbitals, and the Kr virtual levels have been taken from Moore's atomic tables.[17] The 3d hole state levels have been positioned by using the shake-up spectrum of atomic Kr[7] with the same assumptions as for XeF_2.[3] The major assumption is that the Rydberg orbitals in atomic Xe and XeF_2 or in atomic Kr and KrF_2 have the same energy. This assumption leads to good agreement between predicted and observed shake-up energies in the XeF_2 case.[3]

With the molecular orbital diagrams in Figures 3 and 4, we are now in an excellent position to assign the experimental shake-up spectra in Figures 1 and 2. We consider only transitions to the first member of the Rydberg series (i.e., 5s or 5p) because the intensity of the transition to higher members of the Rydberg series has been found to be much weaker.[18] Both the atomic model and Xα calculations predict the same order, while the Xα calculations give considerably better agreement with experiment. By far the most intense peak in the Kr 3d spectrum is peak 1 (at 8.4 eV), which is assigned to the $5\sigma_u \rightarrow 6\sigma_u$* transition. This is analogous to the low-energy transition ($6\sigma_u \rightarrow 7\sigma_u$*) observed in XeF_2 at 8.05 eV.[3] As with XeF_2, both the Xα calculation and atomic model overestimate the energies for this shake-up peak (Table I). In addition to the shake-up energy calculations, we have also used Loubriel's program[14] to calculate molecular shake-up intensities in KrF_2. The $5\sigma_u \rightarrow 6\sigma_u$* transition represents a good test case for this calculation, as it is the only shake-up peak with very well-defined energy and intensity. The agreement between the experimental (9.76%) and calculated (9.82%) intensities is remarkably good. The Xα–SW calculation (Table I) predicts that the next most intense peak will belong to the $3\pi_u \rightarrow 5\pi_u$* transition (3.74%). This is predicted to be at least 10 times more intense than the remaining shake-up transitions. An investigation of the orbital character (Table IV) shows that the $3\pi_u$ orbital is predominantly Kr p in character and the $5\pi_u$* is largely Rydberg p character. Employing the atomic model formalism, we draw an analogy between this transition and the atomic Kr 4p → 5p transition. The fact that this transition has been predicted to be the most intense of the Rydberg type excitations clearly supports the atomic model. The $7\sigma_g \rightarrow 9\sigma_g$* transition, which is analogous to the atomic Kr 4s → 5s transition, is also predicted to be one of the more intense

(16) W. Lotz, *J. Opt. Soc. Am.*, **60**, 206 (1970).
(17) C. E. Moore, *Natl. Bur. Stand. (U.S.), Circ.*, No. 467 (1958).
(18) U. Gelius, *J. Electron Spectrosc. Relat. Phenom.*, **5**, 985 (1974).

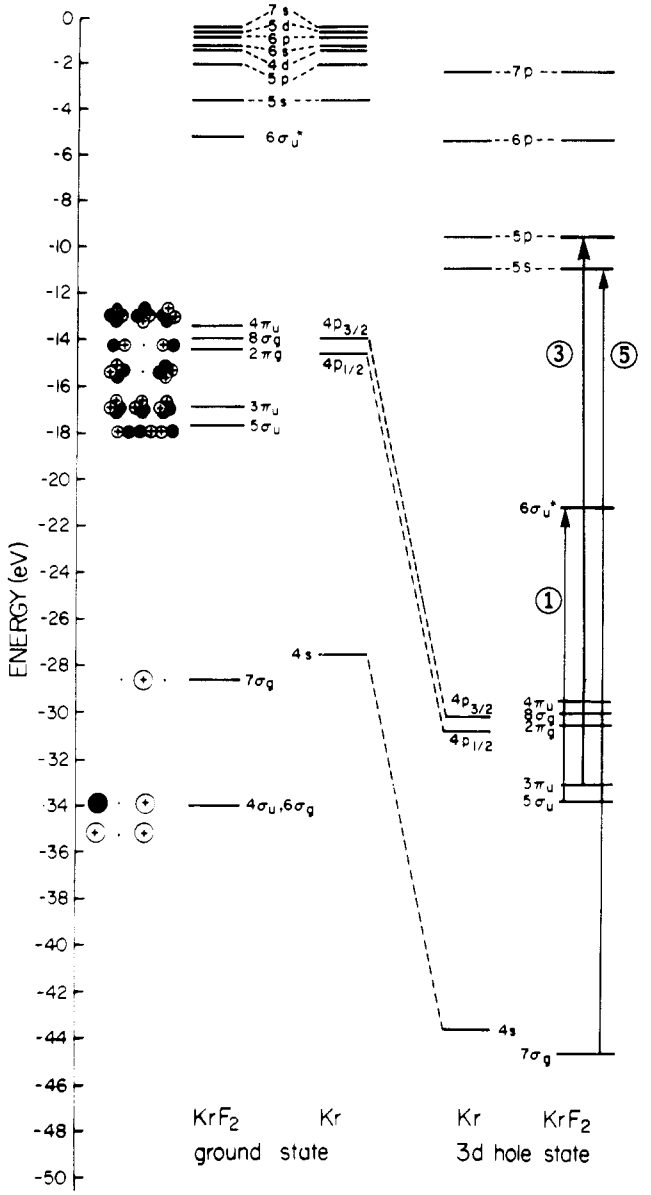

Figure 4. Energy levels for the ground and 3d hole states in KrF_2 obtained by using the atomic model.

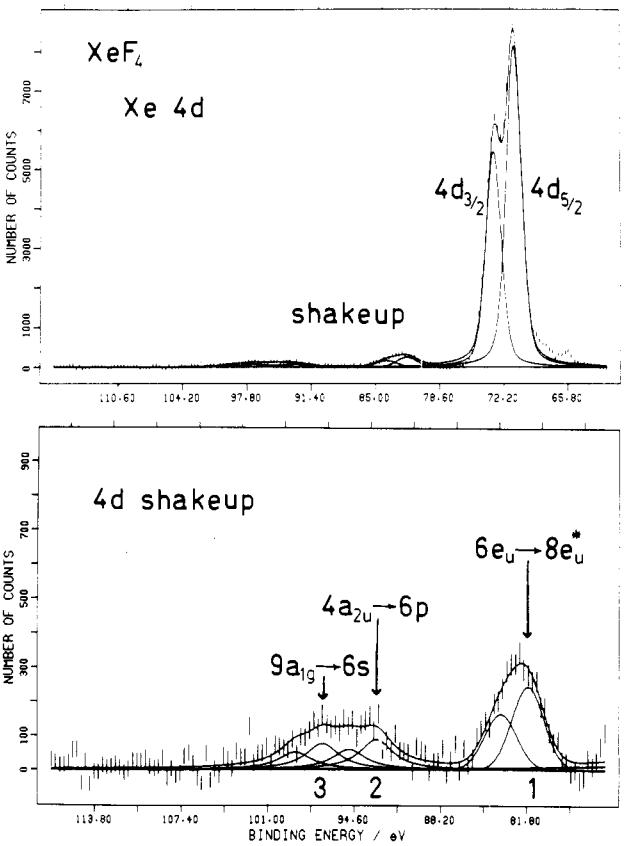

Figure 5. Shake-up spectrum of XeF_4: (a) full scan of the Xe 4d region; (b) blowup of the shake-up region.

Table VII. XeF_4 Xe 4d Core Level Satellite Lines

		energy, eV		
line no.	assignt	obsd	fwhm (intens)[a]	theor
1	$6e_u \rightarrow 8e_u^*$	10.7	2.8 (4.0)	10.2[b]
2	$5a_{2u} \rightarrow 6p$	21.8	3.2 (2.3)	17.5[c]
2	$4a_{2u} \rightarrow 6p$	21.8	3.2 (2.3)	22.3[c]
3	$9a_{1g} \rightarrow 6s$	25.8	3.2 (2.0)	31.8[c]

[a] In percent; relative to main Xe 4d photoline. [b] Reference 20. [c] Atomic model; valence binding energies taken from ref 21.

Rydberg transitions (0.11%).[11] The $5\sigma_u \rightarrow 7\sigma_u^*$ transition is from a Kr p to Rydberg p type orbital, which is again consistent with the atomic model. The other two assignments ($2\pi_g \rightarrow 3\pi_g^*$ and $4\sigma_u \rightarrow 7\sigma_u^*$) were made on the basis of the most intense transitions in the pertinent energy range. Apart from the good agreement between calculated and observed intensities for the $5\sigma_u \rightarrow 6\sigma_u^*$ transition, it is apparent that calculated intensities are not in good agreement with observed values.

The assignment of the F 1s shake-up spectrum (Figure 2) is somewhat more difficult than that of the Kr 3d spectrum since the localized F 1s hole requires a lowering of the symmetry from $D_{\infty h}$ to $C_{\infty v}$. Formally, then, far more transitions are allowed as there are only σ and π type orbitals. Also, the atomic model cannot be applied to the F 1s hole situation, so that all assignments have been based on the Xα–SW energies and intensities. The various assignments and the corresponding energies and intensities have been listed in Table II. As with the Kr 3d spectrum, the only completely unambiguous assignment can be made for the first peak $12\sigma \rightarrow 14\sigma^*$. The agreement between the observed (12.94%) and calculated (12.96%) intensities is excellent, and the percent orbital character (Table V) indicates that this transition is analogous to the $5\sigma_u \rightarrow 6\sigma_u^*$ transition in the Kr 3d hole state. The intensities of the remaining peaks, as was the case in the Kr 3d calculation, have been considerably underestimated. The reason for this is not entirely clear but could in part be due to shake-off limits coincidental with the observed peaks or contributions from inelastic scattering. This would tend to enhance their intensity.

(b) XeF_2 and XeF_4. The greater complexity of the molecular orbital scheme for XeF_4 and XeF_6[19] makes it much more difficult to assign these spectra. Because the F 1s line overlaps the Xe 3d spectrum, we recorded the Xe 4d spectrum (Figure 5). This spectrum can be fitted rather well with three spin–orbit doublets. The transition energies and assignments are summarized in Table VII. In order to make these assignments, we have assumed that the most likely transitions will involve valence orbitals exhibiting considerable Xe p or s character. To facilitate determination of the orbital character, we have performed an Xα–SW calculation on XeF_4. The orbitals with significant Xe character are $4a_{2u}$ (35.2% p), $5a_{2u}$ (31.4% p), $6e_u$ (36.3% p), and $9a_{1g}$ (74.5% s). A recent DVM–Xα calculation on XeF_4[20] has calculated the binding

(19) H. Basch, J. W. Moskowitz, C. Hollister, and D. Hankin, *J. Chem. Phys.*, **55**, 1922 (1971).
(20) G. L. Gutsev and A. E. Smoljar, *Chem. Phys.*, **56**, 189 (1981).

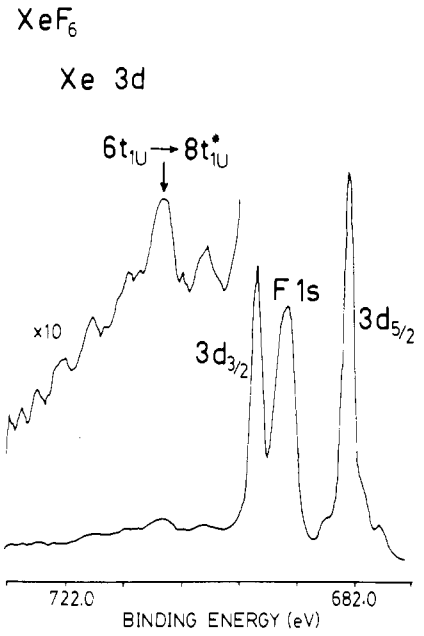

Figure 6. Shake-up spectrum of the Xe 3d orbital in XeF_6. Counts on the Xe $3d_{5/2}$ line total over 3000. The lines are a seven-point smooth to the data.

energy of the lowest unoccupied molecular orbital ($8e_u$*). The monopole selection rules allow transitions to this virtual level from the $7e_u$, $6e_u$, or $5e_u$ valence orbitals. Since only the $6e_u$ valence orbital has appreciable Xe character, we would predict the transition to be $6e_u \rightarrow 8e_u$*. With the eigenvalues obtained from the DVM–Xα calculation, the transition energy is 10.2 eV, which corresponds almost exactly with that observed for peak 1 (10.7 eV). This transition ($6e_u \rightarrow 8e_u$*) is analogous to the lowest energy shake-up peak observed in XeF_2 ($6\sigma_u \rightarrow 7\sigma_u$*).

In lieu of a theoretical calculation dealing with the higher virtual levels in XeF_4, we have used the atomic model to assign peaks 2 and 3. The Rydberg 6s and 6p orbitals of XeF_4 are positioned exactly as they were in XeF_2.[3] The two orbitals containing the majority of the Xe 5p character are the $4a_{2u}$ and the $5a_{2u}$ levels. The energies of the two shake-up transitions ($5a_{2u} \rightarrow 6p$; $4a_{2u} \rightarrow 6p$) can be easily determined via the atomic model in conjunction with the experimental valence binding energies.[21] As is evident in Table VII, the calculated $4a_{2u} \rightarrow 6p$ transition at 22.3 eV is much closer to the observed (21.8 eV) than the $5a_{2u} \rightarrow 6p$ transition (17.5 eV).

Peak 3 has been assigned to the $9a_{1g} \rightarrow 6s$ transition. The $9a_{1g}$ orbital is 74.5% Xe s in character. Hence this shake-up transition is analogous to the atomic Xe 5s → 6s transition. The agreement here is the poorest as one might expect since the atomic model assumes that the Xe 5s orbital shifts the same amount as the predominantly Xe 5p orbitals on core hole formation.

The Xe 3d shake-up spectrum of XeF_6 is presented in Figure 6. It was not possible to obtain a reasonable Xe 4d spectrum because of channeltron degradation. We did not attempt a computer fit of this spectrum because of its complexity and lack of resolution. As with XeF_2 and XeF_4, there is one clearly defined low-energy peak corresponding to the first bonding to antibonding transition. The shake-up peak associated with the Xe $3d_{3/2}$ level has been assigned on the spectrum. The analogous peak resulting from Xe $3d_{5/2}$ ionization is hidden beneath the F 1s peak. A recent DVM–Xα calculation on XeF_6[20] has located the lowest unoccupied molecular orbital ($8t_{1u}$*). Monopole selection rules allow transitions from the $5t_{1u}$, $6t_{1u}$, and $7t_{1u}$ valence orbitals. An investigation of the orbital character from our Xα–SW calculation[22] shows that of these three orbitals, only the $6t_{1u}$ has significant Xe p character (28.8%). The excitation energy calculated for the $6t_{1u} \rightarrow 8t_{1u}$* transition by using both SW–Xα[23] and DVM–Xα[20] calculations is 11.8 eV.

Acknowledgment. We thank the NSERC of Canada for financial support and R. Lazier for technical assistance.

Registry No. KrF_2, 13773-81-4; XeF_4, 13709-61-0; XeF_6, 13693-09-9.

(21) C. R. Brundle, M. B. Robin, and G. R. Jones, *J. Chem. Phys.*, **52**, 3383 (1970).
(22) D. J. Bristow, Ph.D. Thesis, University of Western Ontario, 1982.
(23) E. W. Phillips, J. W. D. Connolly, and S. B. Trickey, *Chem. Phys. Lett.*, **17**, 203 (1972).

Contribution from the Department of Chemistry, University of Washington, Seattle, Washington 98195

Thermodynamic Properties of Iron(III) Oxychloride

N. W. GREGORY

Received October 6, 1982

Vapor-phase concentrations of Fe_2Cl_6(g) above solid mixtures, formed by interaction of Fe_2O_3 and $FeCl_3$, have been measured spectrophotometrically in the range 465–560 K. The equilibrium behavior, assumed to characterize the reaction 6FeOCl(s) = $2Fe_2O_3$(s) + Fe_2Cl_6(g), projects pressures at higher temperatures which, within experimental uncertainty, agree with manometric data obtained with a Pyrex diaphragm gauge (580–670 K) and with earlier manometric measurements (660–770 K) reported by Stirnemann. A least-squares treatment of the combined absorbance and manometric data, using an estimated equation for $\Delta C_p°$, gives the following relationship: $\ln P_{Fe_2Cl_6(atm)} = -12.89 \ln T + 0.01755T - 5.827 \times 10^{-6}T^2 - 18550T^{-1} + 101.59$. Pressures given by this equation are substantially higher than those predicted for this reaction from thermodynamic constants reported by others. Possible reasons for the discrepancy are discussed.

In a recent paper Stuve, Ferrante, Richardson, and Brown[1] report heat capacity data for $FeCl_3$(s) (4.6–300 K) and for FeOCl(s) (6–700 K) and a value for the standard enthalpy of formation of FeOCl(s) at 25 °C. The last value is based on measured heats of solution of FeOCl(s) in aqueous HCl and heats of solution and the standard enthalpy of formation of $FeCl_3$(s).[2,3] Standard thermodynamic constants are tabulated for FeOCl(s) at various temperatures. When used together with thermodynamic constants reported in ref 3 for

(1) Stuve, J. M.; Ferrante, M. J.; Richardson, D. W.; Brown, R. R. *Rep. Invest.—U.S., Bur. Mines* **1980**, *RI*-8420.
(2) See also: Schafer, H.; Wittig, F. E.; Jori, M. *Z. Anorg. Allg. Chem.* **1956**, *287*, 61.
(3) "JANAF Thermochemical Tables", Supplement; Dow Chemical Co.: Midland, MI, June 30, 1965.

0020-1669/83/1322-2677$01.50/0